AGU PUBLICATIONS

Tectonics

RESEARCH ARTICLE
10.1002/2014TC003576

Key Points:
- New crustal seismicity, focal mechanism data from local network for the Pamir
- New comprehensive neotectonic map for the Pamir
- Seismic deformation is dominated by N-S shortening and westward extrusion

Supporting Information:
- Readme
- Table S1
- Table S2
- Figure S1
- Figure S2
- Figure S3

Correspondence to:
B. Schurr,
schurr@gfz-potsdam.de

Citation:
Schurr, B., L. Ratschbacher, C. Sippl, R. Gloaguen, X. Yuan, and J. Mechie (2014), Seismotectonics of the Pamir, *Tectonics*, *33*, 1501–1518, doi:10.1002/2014TC003576.

Received 17 MAR 2014
Accepted 27 JUN 2014
Accepted article online 16 JUL 2014
Published online 5 AUG 2014

Seismotectonics of the Pamir

Bernd Schurr[1], Lothar Ratschbacher[2], Christian Sippl[1,3], Richard Gloaguen[2,4], Xiaohui Yuan[1], and James Mechie[1]

[1]Deutsches GeoForschungsZentrum GFZ, Potsdam, Germany, [2]Institut für Geologie, Technische Universität Bergakademie Freiberg, Freiberg, Germany, [3]Now at Research School of Earth Sciences, Australian National University, Canberra, ACT, Australia, [4]Now at Helmholtz-Institut Freiberg für Ressourcentechnologie, Freiberg, Germany

Abstract Based on a 2 year seismic record from a local network, we characterize the deformation of the seismogenic crust of the Pamir in the northwestern part of the India-Asia collision zone. We located more than 6000 upper crustal earthquakes in a regional 3-D velocity model. For 132 of these events, we determined source mechanisms, mostly through full waveform moment tensor inversion of locally and regionally recorded seismograms. We also produced a new and comprehensive neotectonic map of the Pamir, which we relate to the seismic deformation. Along Pamir's northern margin, where GPS measurements show significant shortening, we find thrust and dextral strike-slip faulting along west to northwest trending planes, indicating slip partitioning between northward thrusting and westward extrusion. An active, north-northeast trending, sinistral transtensional fault system dissects the Pamir's interior, connecting the lakes Karakul and Sarez, and extends by distributed faulting into the Hindu Kush of Afghanistan. East of this lineament, the Pamir moves northward *en bloc*, showing little seismicity and internal deformation. The western Pamir exhibits a higher amount of seismic deformation; sinistral strike-slip faulting on northeast trending or conjugate planes and normal faulting indicate east-west extension and north-south shortening. We explain this deformation pattern by the gravitational collapse of the western Pamir Plateau margin and the lateral extrusion of Pamir rocks into the Tajik-Afghan depression, where it causes thin-skinned shortening of basin sediments above an evaporitic décollement. Superposition of Pamir's bulk northward movement and collapse and westward extrusion of its western flank causes the gradual change of surface velocity orientations from north-northwest to due west observed by GPS geodesy. The distributed shear deformation of the western Pamir and the activation of the Sarez-Karakul fault system may ultimately be caused by the northeastward propagation of India's western transform margin into Asia, thereby linking deformation in the Pamir all the way to the Chaman fault in the south in Afghanistan.

1. Introduction

Crustal deformation during orogeny is often complex because mountain belts are affected by a variety of forces and boundary conditions. Tectonic forces from plate convergence cause crustal thickening by thrusting and folding. Material flow from the orogenic interior to the exterior may be by pure wrenching (lateral escape) [e.g., *Tapponnier et al*., 1982], transpression and/or transtension (lateral extrusion) [e.g., *Ratschbacher et al*., 1991], and/or by purely gravitational forces, causing orogenic collapse and crustal extension [e.g., *Dewey*, 1988]. Exogenic factors such as climate and its influence, e.g., on erosion, may also influence deformation [e.g., *Pavlis et al*., 1997; *Beaumont et al*., 2001]. In addition, subcrustal processes such as lithospheric-scale underthrusting, subduction, or delamination [*Bird*, 1979] may exert stresses on the upper crust, depending on whether mantle lithosphere and upper crust are coupled [e.g., *Flesch et al*., 2005; *Copley et al*., 2011; *Flesch and Bendick*, 2012]. Herein, we investigate how the seismogenic crust of the Pamir in the northwestern part of the India-Asia collisional belt is deforming under its given boundary conditions.

The Pamir occupies an orographic node northwest of Tibet, between the Tarim and Tajik-Afghan basins, where the Hindu Kush, Karakorum, western Kunlun Shan, and Tian Shan coalesce (Figure 1). It formed north of the Western Himalayan Syntaxis, on the Asian (retro)continent, and accommodated a higher amount of Cenozoic crustal shortening over a shorter north-south distance than Tibet [*Schmidt et al*., 2011; *van Hinsbergen et al*., 2011]. Its shape is a northward convex orocline. The Pamir region, including the neighboring Hindu Kush, is unique in featuring intense intermediate depth (~90–250 km) seismicity in an intracontinental setting, testifying to vigorous geodynamic processes in the mantle below. These deep earthquakes form thin inclined planes (Figure 1) [*Billington et al*., 1977; *Pegler and Das*, 1998; *Sippl et al*., 2013a], reminiscent of

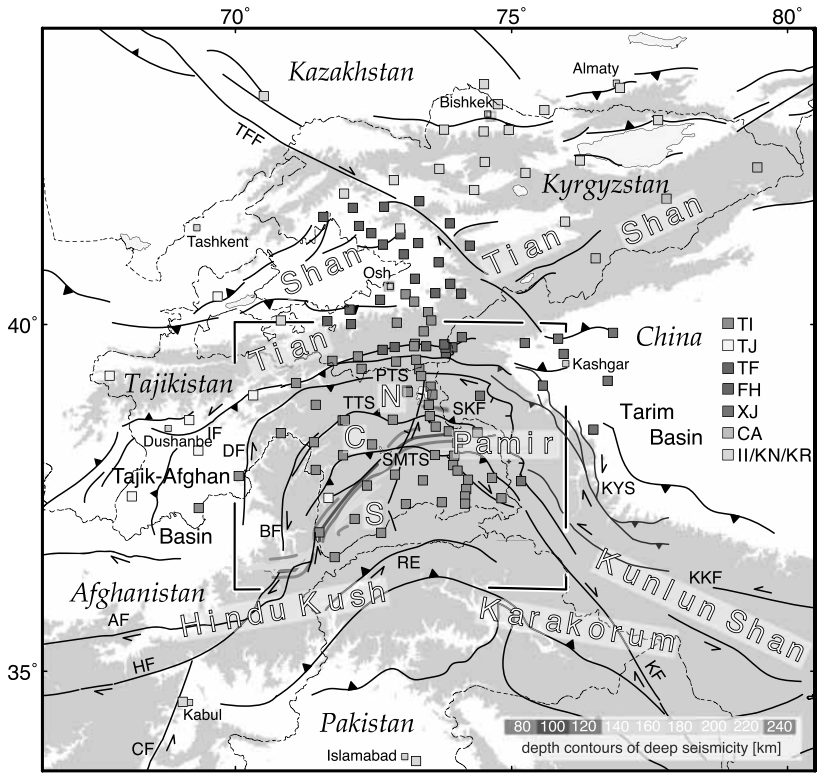

Figure 1. Tectonic overview map of western Central Asia with main neotectonic structures drawn as black lines. Abbreviations are AF = Andarob fault, BF = Badakhshan fault, CF = Chaman fault, DF = Darvaz fault, HF = Herat fault, KKF = Karakax fault, KF = Karakorum fault, KYS = Kashgar-Yecheng transfer system, IF = Illiac fault, RE = Reshun-Hunza fault system, PTS = Pamir thrust system, SKF = Sarez-Karakul fault system, SMTS = Sarez-Murghab thrust system, TFF = Talas Ferghana fault, and TTS =Tanymas thrust system. Regions above 2500 m sea level are shaded. Colored squares show seismic stations used in the analysis presented here. Networks TI, FH, and TF were temporary deployments between 2008 and 2010; the rest are permanent stations from various networks. The colored contours mark the location and depth of the Pamir-Hindu Kush deep seismic zone. Box shows the map extent displayed in Figure 3.

Wadati-Benioff zones known from oceanic subduction, and were consequently interpreted as evidence for continental subduction [e.g., *Burtman and Molnar*, 1993]. More recent studies, employing seismic imaging from a local network [*Schneider et al*., 2013; *Sippl et al*., 2013b], show that the cold Asian mantle lithosphere under the Pamir indeed seems to descend, but with only the lower crust attached to it. Shortening due to Pamir's northward indentation is currently focused along a thrust system along its northern perimeter, the Pamir thrust system (Figures 1 and 2), where a significant portion of the total India-Asia convergence at this longitude is accommodated [*Reigber et al*., 2001; *Mohadjer et al*., 2010; *Zubovich et al*., 2010; *Ischuk et al*., 2013].

We use a large data set of earthquake locations and source mechanisms from a 2 year seismic deployment to characterize, together with published GPS measurements and a reassessment of the Cenozoic structures, the Pamir's current deformation field (Figures 1–4). Previous seismotectonic studies where either local [*Hamburger et al*., 1992; *Strecker et al*., 1995; *Lukk et al*., 1995; *Arrowsmith and Strecker*, 1999] or based on teleseismic data [*Burtman and Molnar*, 1993; *Fan et al*., 1994], which sample only the largest events that do not provide the spatial resolution necessary to address deformation at the scale of individual faults. In our analysis of Pamir's active tectonics, we are particularly interested in how far the surface deformation pattern coincides with the structures built up over the last ~50 Myr of India-Asia convergence and is coupled to or caused by the large-scale subcrustal processes.

2. Tectonic Setting

To a first order, the Pamir lithosphere consists of three tectonostratigraphic units, which originated from the accretion of microcontinents, arcs, and subduction-accretion complexes to Asia during the Paleozoic and

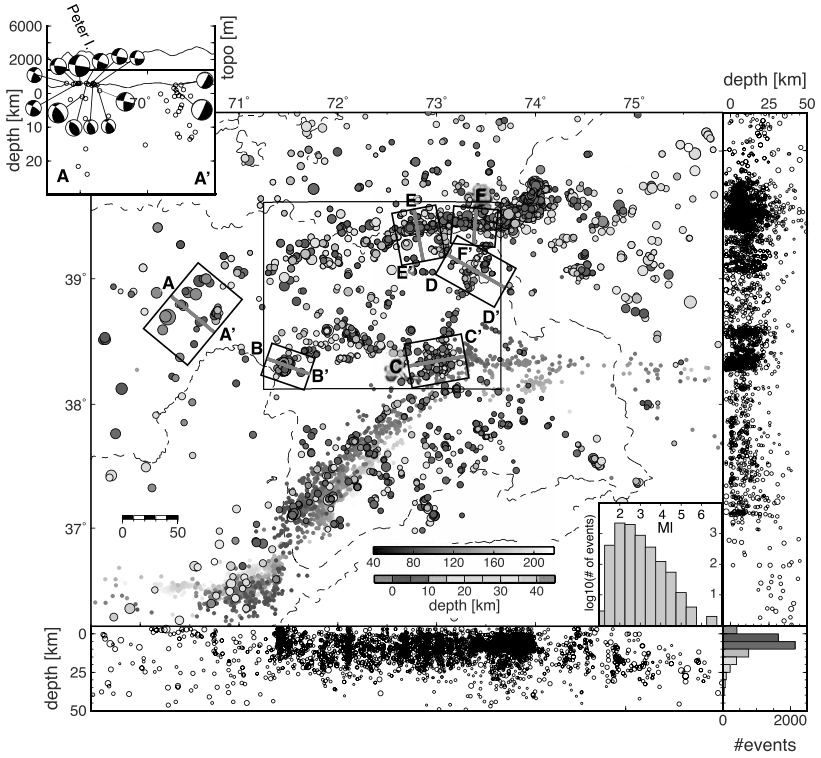

Figure 2. Seismicity map and cross sections of the Pamir region. Dashed line marks political boundaries. Earthquakes are marked as circles, color coded differently for crustal (rainbow) and intermediate-depth (gray) seismicity. Intermediate-depth seismicity is taken from *Sippl et al.* [2013a]. In latitudinal and longitudinal cross sections the entire seismicity is projected. The grey histogram bins the number of crustal events per magnitude; and the colored histogram in the lower right corner counts the number of events in 5 km depth bins. Most crustal seismicity occurs in the upper 15 km of the crust. Section across the Peter I. range, including possible shallow detachment faulting events, is plotted in upper left corner. Other cross sections marked on map are shown in Figure 6, of which the map extent is outlined by the large box.

Early Mesozoic [e.g., *Burtman and Molnar*, 1993; *Schwab et al*., 2004], dividing the Pamir into the North, Central, and South Pamir (Figure 1). The Cenozoic Pamir thrust system confines the North Pamir along its northern, frontal perimeter, overprinting the North Pamir Kunlun suture zone; its southern boundary is the Tanymas thrust system, reactivating the Tanymas-Jinsha suture zone. The Sarez-Murghab thrust system separates the Central and South Pamir, reactivating the Rushan-Pshart suture zone.

As the Pamir moved north, it thrusted over what once connected the Tajik-Afghan basin with the Tarim basin (Figure 1). Today, the last vestige of this vanishing piece of crust is the Alai valley, squeezed between the North Pamir and the South Tian Shan (Figure 3). The up to 7100 m high Trans Alai range, which bounds the Alai valley to the south, is the leading edge of the thrust-fold belt of the North Pamir. The Pamir thrust system currently absorbs most of the Pamir's convergence with the Tian Shan, which has been quantified in GPS campaigns [*Reigber et al*., 2001; *Mohadjer et al*., 2010; *Zubovich et al*., 2010; *Ischuk et al*., 2013] to ~13–15 mm/yr (Figure 4b). This is more than one third of the total convergence between India and Asia at this longitude (~34 mm/yr) and makes the Pamir thrust system one of the regions with the highest strain rates in the entire India-Asia collision zone. The sparseness of GPS measurement points, however, does not allow constraining where and how this strain accumulated across the tens of kilometer-wide swath that contains the faults and folds of the Pamir thrust system. The leading thrust-fold belt widens west of the Alai valley, where the Peter I. range (Figures 2 and 3) consists of Tajik-Afghan basin sedimentary rocks wedged between the Pamir and the Tian Shan. Seismicity indicates deformation of both the sedimentary rocks and the southeast dipping basement below [*Hamburger et al*., 1992]. One of the largest historical earthquakes in our study region, the 1949 *M* 7.4 Khait earthquake (Figure 3 and 4b), occurred on the Vakhsh thrust system (Figure 3) or on faults already in the Tian Shan [*Leith and Simpson*, 1986a; *Nikonov*, 1988; *Evans et al*., 2009].

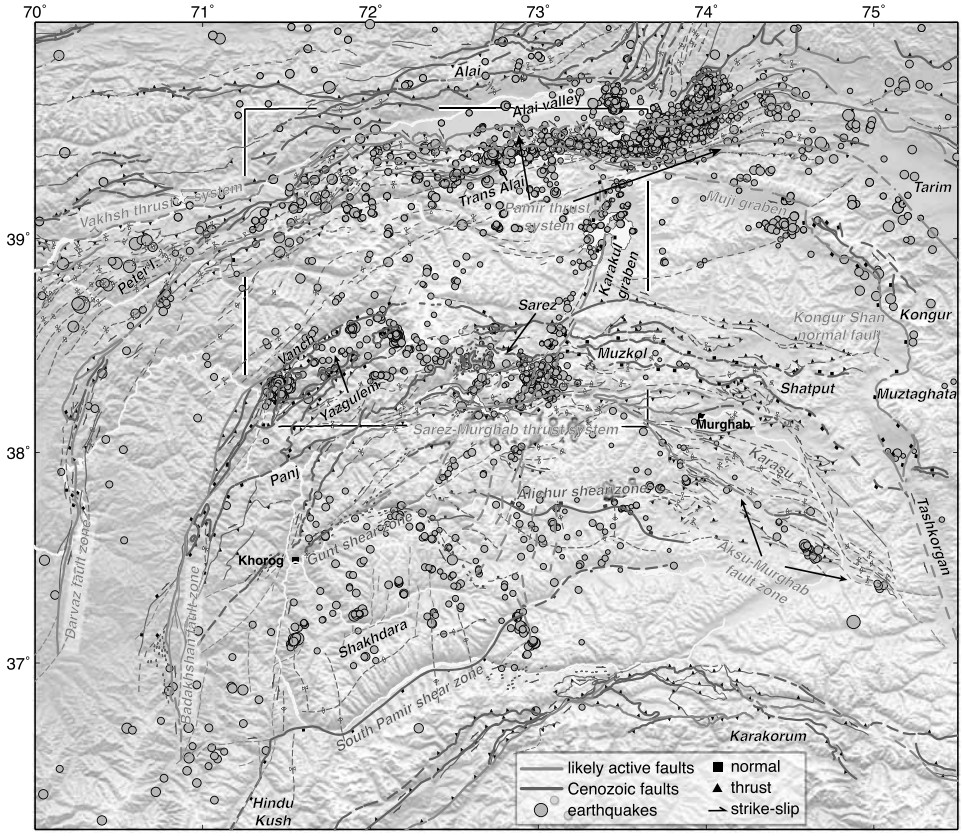

Figure 3. Cenozoic tectonic map of the Pamir and South Tian Shan; see text for sources of the compiled structures. Neotectonic structures are in red. Green circles are crustal earthquakes detected between 2008 and 2010. The yellow star marks the epicenter of the 1949 *M* 7.4 Khait earthquake in the Vakhsh thrust system. Box shows the map extent displayed in Figure 6.

Strike-slip systems accommodate the Pamir's northward advance laterally (Figures 1 and 2). To the west, the sinistral transpressive Darvaz fault zone separates the Pamir from the Tajik-Afghan basin. Currently, shear between the western Pamir and the Tajik-Afghan basin amounts to ~10 mm/yr measured by GPS [*Ischuk et al*., 2013], but the sparseness of GPS points does not allow to constrain its distribution or localization. *Trifonov* [1978] reported a Quaternary slip rate of ~13 mm/yr for the Darvaz fault zone from offset features, but this estimate has significant uncertainty due to the difficulty in dating the features. To the east, where the Pamir borders the Tarim basin, dextral shear occurs along the Karakorum fault system, which probably links with the Sarez-Murghab thrust system via the Aksu-Murghab fault zone, and the dextral transpressive Kashgar-Yecheng fault system (Figures 1 and 2) [*Cowgill*, 2010]. The latter links shortening in the western Kunlun Shan and along the Pamir thrust system. Since ~5 Ma [*Sobel et al*., 2011] and up to now [*Zubovich et al*., 2010], the Pamir and the Tarim basin have been moving north at about the same speed, rendering the transform component mostly inactive [*Cowgill*, 2010]. These strike-slip systems possibly accumulated ~300 km northward displacement of the Pamir relative to Tibet. The thickened crust of the Pamir may have accommodated a similar amount of internal shortening [*Burtman and Molnar*, 1993; *Schmidt et al*., 2011].

3. Crustal Seismicity and Source Mechanism

We present seismicity recorded between 2008 and 2010 on temporary seismic networks deployed in Tajikistan and Kyrgyzstan [*Haberland et al*., 2011; *Mechie et al*., 2012] and on supplementary regional permanent stations (Figure 1). Taking the earthquake catalog of *Sippl et al*. [2013a] as basis, we extracted the crustal events (depth $<$40 km). In addition to their processing, we relocated these events in a new 3-D velocity model [*Sippl et al*., 2013b] that accounts for the large variations of crustal structure and topography encountered in our study area (e.g., contrast between the Tajik-Afghan depression and the thick Pamir Plateau, Figure S1), allowing better

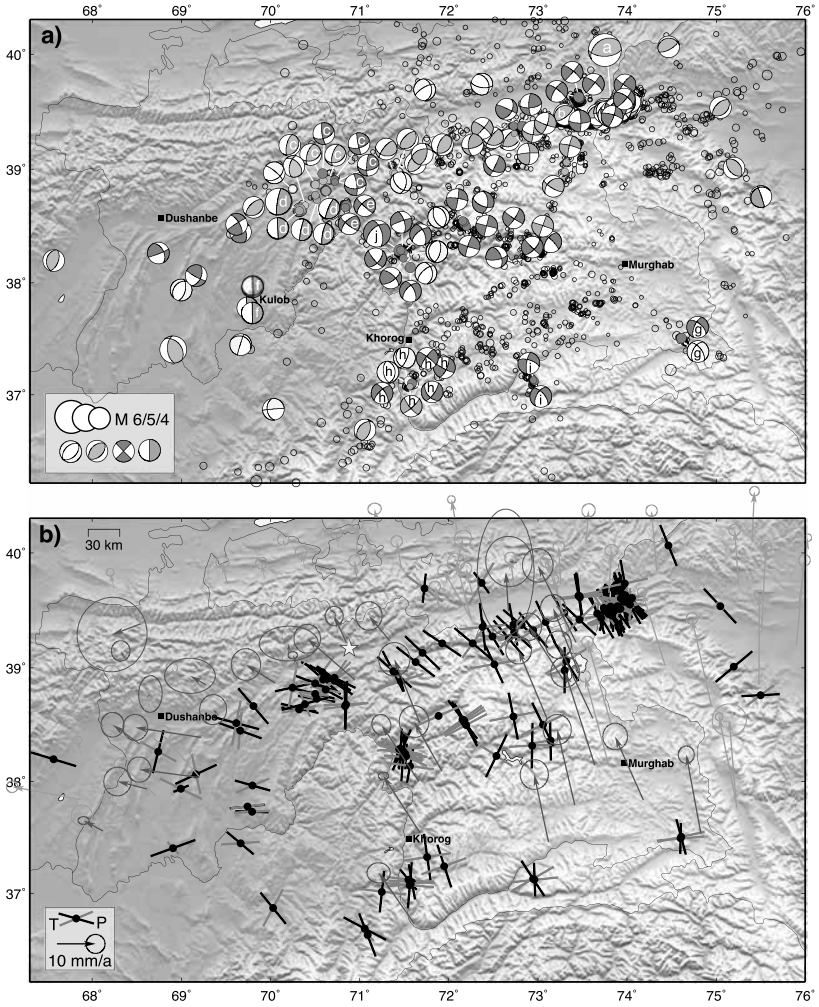

Figure 4. (a) The double-couple component of the moment tensors determined in this study plotted on a topographic map. Color coding is according to faulting type (red = strike slip, yellow = normal, and blue = thrust). Faded colors indicate mechanisms determined by first-motion polarities, strong colors by waveform modeling. Green-colored mechanisms are a subset of the thrust type (blue) with one very shallow (<10°) nodal plane, which we interpret as detachment faults. Letters mark events mentioned in text. (b) Pressure (black) and tension axes (red) from moment tensors and GPS velocity vectors [*Zubovich et al*., 2010; *Ischuk et al*., 2013]. The yellow star marks the epicenter of the 1949 *M* 7.4 Khait earthquake.

constrained hypocentral depths (Figure S2). We then used the double-difference relocation algorithm [*Waldhauser and Ellsworth*, 2000] with the same 3-D velocity model to refine the relative locations. Figure 2 displays epicenters and latitudinal and longitudinal cross sections of 6082 earthquakes with local magnitudes between 1.1 and 6.7 (see frequency-magnitude distribution in Figure 2). About half of the earthquakes pertain to the aftershock series of the largest event, the 2008 M_w 6.7 Nura earthquake, at the eastern end of the Alai valley.

The relocation in the 3-D velocity model tightens the depth distribution at shallower level compared to the original locations based on a 1-D model from *Sippl et al*. [2013a] (Figure S2). The earthquakes now span mostly the depth range of the upper 15 km of the crust (e.g., histogram in Figure 2), representing a normal seismogenic thickness of the brittle crust for the Pamir. Only in the SW and NE corners of our study region, i.e., under the Tarim basin and Hindu Kush, earthquakes appear to reach deeper (Figure 2) possibly indicating thick-skinned deformation of basement rocks under thick sediments. However, these earthquakes are also outside the footprint of our network, and hence, their depths might not be well constrained.

We derived earthquake source mechanisms in two ways. For 120 events, which were strong enough (M_w 3.2–6.7) to produce sufficient signal at long periods (>10 s), we inverted complete local and regional

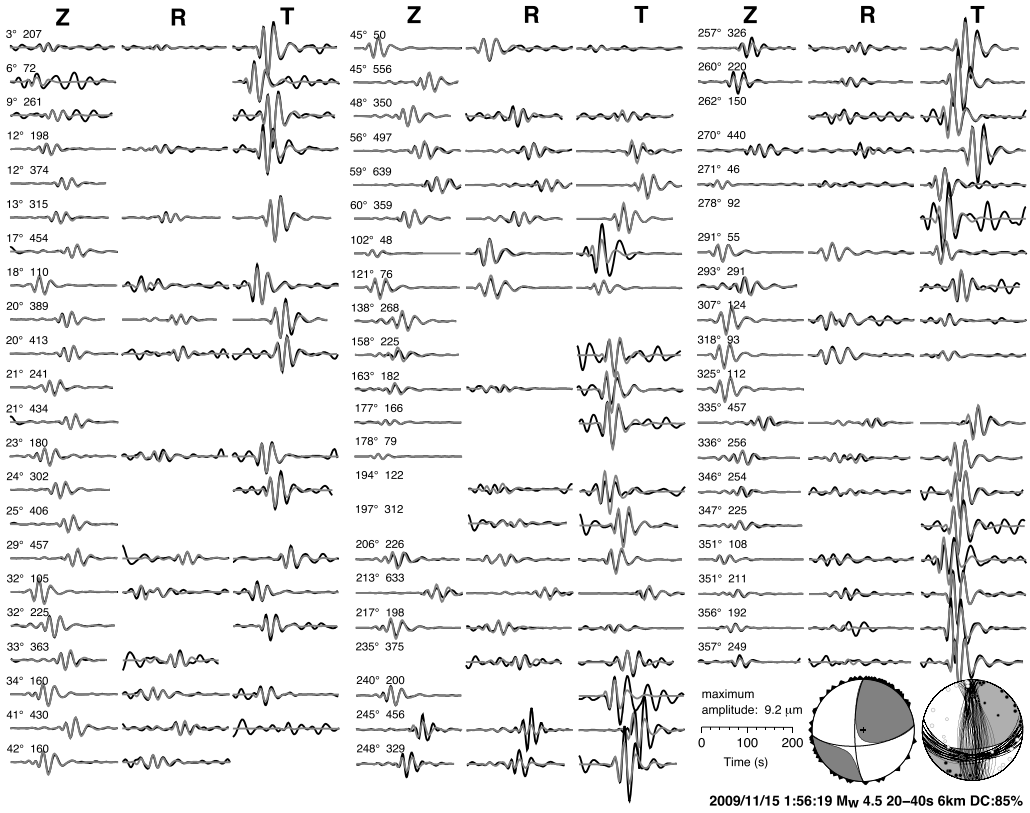

Figure 5. Example for the determination of source parameters for a moderate M_W 4.5 earthquake. If possible, we modeled (red) complete local and regional long-period waveforms (black, here in the 20–40 s pass band). First number above each seismogram is event-station azimuth in degrees; second number is event-station distance in km. Displayed waveforms are sorted by azimuth, showing how well the mechanism is constraint by amplitude variations on the vertical (*Z*), radial (*R*), and transverse (*T*) components. For some smaller events, which did not show enough signal at long periods but had good azimuthal station distribution, we mapped the first-motion polarities to obtain the nodal planes (example for the same event at lower right, filled circles "up," open circles "down"). DC = double-couple component.

(up to ~800 km epicentral distance) displacement seismograms from the temporary and permanent broadband stations in the time domain for the deviatoric moment tensor [*Schurr and Nábělek*, 1999]. For these events, the large number of stations at a variety of azimuths and distances constrains the solution very well (Figure 5). For 12 additional events, which were too small for moment tensor inversion, yet had good enough coverage in station azimuth and distance to constrain the two nodal planes well, we determined fault plane solutions from first-motion polarities [*Hardebeck and Shearer*, 2002] (Figure 5). Figure 4 visualizes the double-couple source mechanisms and associated *P* and *T* axes. Source parameters are available as Tables S1 and S2 in the supporting information.

4. Cenozoic and Neotectonic Fault and Fold Map

We plotted the epicenters over a new, simplified tectonic map of the Pamir and the South Tian Shan (Figure 3). The map illustrates the distribution of faults and folds that we interpret to have been active in the Cenozoic in blue; it highlights neotectonic (Late Cenozoic, mostly active) structures in red. We interpreted the Cenozoic faults and folds from the classified 1:200,000 geologic maps of the Tajik Soviet Socialist Republic, their stratigraphic revision on the scale of 1:500,000 [*Vlasov et al*., 1991], and the 1:850,000 Geological and Mineral Resource Map of Afghanistan [*Doebrich and Wahl*, 2006]. We simplified the structures of the Chinese Pamir from *Robinson et al*. [2007], *Fu et al*. [2010], and *Li et al*. [2012] and those of the Hindu Kush and Karakorum from *Searle and Khan* [1996] and *Zanchi et al*. [2011]. The structures of the southwestern Pamir (Shakhdara and Alichur domes and their surroundings; Figure 3) were modified from *Stübner et al*. [2013a]. We used satellite images, digital elevation models, and fieldwork in the course of nine expeditions to ground

check the interpretations. The fieldwork results, which scrutinized ~60% of the Tajik Tian Shan and Pamir, the southern Tian Shan of Kyrgyzstan, and the Wakhan and Badakhshan of Afghanistan, will be reported in combination with the remote sensing tectonic-geomorphologic analysis in detail elsewhere (see *Stübner et al*. [2013a] for a published example). Whereas the assessment of the Cenozoic age of the Pamir structures is based on a substantial geothermochronologic database (see *Schmidt et al*. [2011], *Stearns et al*. [2013], and *Stübner et al*. [2013b] for published examples), the timing of Cenozoic structures in the Tian Shan is mostly based on the involvement of Mesozoic and Cenozoic rocks in the deformation. We classified structures as neotectonic (likely active), when we observed fault scarps, offset geomorphologic features and unconsolidated fault gouge and cataclasite; Figure 6 illustrates active sinistral-normal fault scarps along the southern segment of the Sarez-Karakul fault system (Figure 1) ([*Strecker et al*., 1995] for active deformation features along its northern segment) and dextral-oblique thrusts along the Sarez-Murghab fault zone.

Cenozoic deformation is spectacularly partitioned spatially. In the South Tian Shan, forethrust and back thrust prevail; several of the east trending faults have a dextral strike-slip component, and of the northeast striking faults, in the Alai range northeast of the Alai valley, a sinistral component. The Pamir thrust system has an active thrust front, the Vakhsh thrust system, that extends into the dextral-reverse lateral ramp of the Illiac fault zone, bounding the thrust-fold belt of the Tajik-Afghan basin in the north (Figure 1). The Vakhsh thrust system, and its eastward continuation along the southern Alai valley, is a shallow dipping décollement along Jurassic evaporites; it has detachment folds in the hanging wall. Recent activity along the sinistral transpressive Darvaz fault zone, exemplified by offset streams, likely extends into the rear of the Pamir thrust system, where Jurassic to Paleozoic basement rocks are thrust over Cretaceous and Tertiary strata. The active strands of the Trans Alai range connect via sinistral- and dextral-transpressive conjugate jogs to the forethrust and back thrust that rim the Tarim basin (Figures 1, 2, and 5).

Cenozoic deformation reemerges south of the rigid North Pamir in the Central Pamir (Figure 3). Normal-shear detachments, rimming the Central Pamir gneiss domes, from west to east the Yazgulem, Sarez, Muzkol, and Shatput domes, cut older large displacement nappes [*Rutte et al*., 2013]. The Tanymas thrust system in the north, mostly involving back thrusts in its eastern segment, and the Sarez-Murghab thrust system in the south border these Miocene domes [*Schmidt et al*., 2011; *Stearns et al*., 2013; *Rutte et al*., 2013]. The active Sarez-Murghab thrust system, traced by unconsolidated fault gouges and cataclasites, and scarps, interacts with the Aksu-Murghab dextral strike-slip fault zone of the southeastern Pamir [*Strecker et al*., 1995]. The active, dextral-transpressive Badakhshan fault zone can be traced from central Badakhshan, Afghanistan, across the Panj River to the northern margin of the Yazgulem dome.

The South Pamir again shows distinct Cenozoic deformation (Figure 3). The southwestern Pamir of Tajikistan and Afghanistan features the doubly vergent, composite Shakhdara-Alichur extensional gneiss domes [*Stübner et al*., 2013a, 2013b]; they are separated by a low-strain horst. Top-to-SSE, noncoaxial, pervasive flow over the ≤4 km thick South Pamir shear zone exhumed crust from 30 to 40 km depth in the ~250 × 80 km Shakhdara dome; the top-to-NNE Alichur shear zone exposed upper crustal rocks in the ~125 × 25 km Alichur dome (Figure 3). The Gunt shear zone bounds the Shakhdara dome in the north and separates a zone of ~ north-south extension (the Shakhdara dome) in the south from a zone with approximately north-south shortening and dextral strike slip in the north. The dextral Gunt shear zone is active and connects via distributed shear with the Sarez-Murghab thrust system. Doming started at ~20 Ma along the Gunt normal-shear zone and the bulk of exhumation occurred by approximately north-northeastward extrusion of the footwall of the crustal-scale South Pamir normal-sense shear zone along the southern Shakhdara dome boundary from ~18–15 Ma to ~2 Ma, resulting in ≤90 km approximately northwest-southeast extension. The southeastern Pamir features a Tertiary thrust-fold belt, cut by local active dextral strike-slip faults (Aksu-Murghab fault zone), and the northeastern Pamir, Kongur Shan, and Tashkorgan normal fault systems in China [*Strecker et al*., 1995; *Robinson et al*., 2007].

The active Sarez-Karakul sinistral-normal fault system occupies the meridian axis of the Pamir (Figure 3). Best expressed between the lakes Karakul and Sarez, it interacts with the Pamir thrust system and stretches with distributed deformation into the Wakhan of Afghanistan. Across the central and western Shakhdara dome, it likely connects with approximately NNE trending, active, sinistral faults in the Hindu Kush of Badakhshan. This sinistral system appears to be cut off from the Chaman strike-slip fault system of Afghanistan by the northeast trending dextral Andarob and Herat fault zones (Figure 1). One of the most striking features of Afghan Pamir is the subparallel strike of the active, oppositely slipping Darvaz and Badakhshan fault zones. This resembles the interaction of the dextral Karakorum and sinistral Karakax fault

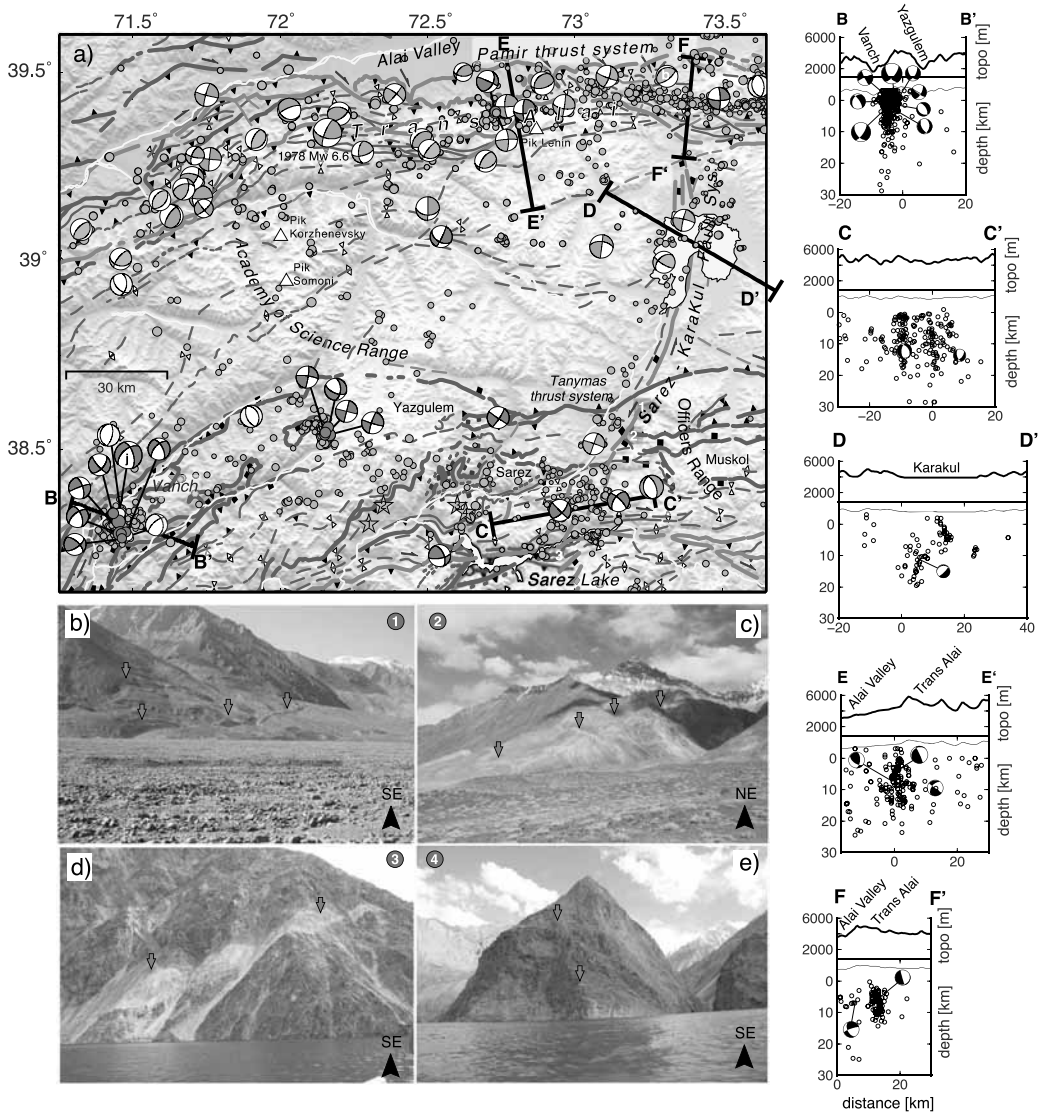

Figure 6. (a) Close-up of the tectonic map in the northwestern quadrant of our study region framed roughly by the Pamir thrust system in the north, the Sarez-Karakul fault system in the east, and the Vanch-Lake Sarez area in the south. Colored beach balls are the same as in Figure 4a; grey beach balls are from the global CMT moment tensor project [*Dziewonski et al*., 1981; *Ekström et al*., 2012] for the years between 1976 and 2008. Letters mark events mentioned in text. Green stars mark possible locations of the 1911 *M* 7.7 Sarez earthquake based on intensity reports (1: *Ambraseys and Bilham* [2012], 2 + 3: *Bindi et al*. [2013], and the Global Instrumental Earthquake Catalogue-International Seismological Centre global earthquake catalog 4: *Storchak et al*. [2013]). Five depth profiles are marked on map and plotted on the right side. (b) Sinistral-normal slip fault scarps along the active southern strand of the Lake Karakul graben system. (c) Cascade of range front normal faults along the active southern strand of the Lake Karakul graben system. (d) Pulverized fault gouge in dextral-reverse thrust imbricate in Cretaceous granite along the likely active Sarez-Murghab thrust system, southern shore of Lake Sarez. (e) Stack of thrusts (granite over granite and granite over possible Tertiary conglomerate) with ultracataclasite layers, likely active Sarez-Murghab thrust system, southern shore of Lake Sarez. Numbers 1–4 in Figures 6b–6e locate the photographs in the map of Figure 6a.

systems in northwestern Tibet (Figure 1). The Tirich Mir and Reshun fault systems, with several active strands, bound the Afghan Hindu Kush and Pamir south of our study area.

5. Results

As with the Cenozoic deformation structures, seismicity in the Pamir is spectacularly partitioned spatially and occurs along well-defined zones (Figures 2–4 and 6). A band of earthquakes outlines Pamir's northern

perimeter, whereas its eastern and western flanks exhibit only sparse and more diffuse seismicity. Active structures occur in the central and western part of the orogenic interior but do not outline the major Cenozoic structural grain, namely, the approximately east trending normal and thrust/shear zones. Instead, the seismicity showcases east-west extension together with north-south shortening, as exemplified by the Sarez-Karakul fault system, and a near absence of thrust-reverse fault solutions.

5.1. Pamir Margins

At the eastern termination of the Alai valley, where the Pamir collides with the Tian Shan, an elongated cluster of well over 3000 earthquakes marks the 2008 M_w 6.7 Nura earthquake (a in Figure 4a) and its aftershocks (Figures 1–3) [*Krumbiegel et al*., 2011]. These occurred in a region where the Pamir thrust system widens and merges with the mostly top-to-S thrusts of the Chinese Tian Shan and the mostly top-to NE thrusts of the northern part of the Chinese Pamir at the western tip of the Tarim basin. In contrast to the mapped thrusts in the Trans Alai range, the faults in the Tian Shan northeast of the Alai valley are steep, thick-skinned, northeast striking reverse faults that only locally carry Mesozoic-Cenozoic basin strata in their hanging wall (e.g., Kichi-Karakol basin just north of the Alai valley); the northeast strike, unusual for the Tian Shan, has been attributed to counterclockwise rotation in the far field of the Talas-Ferghana fault zone [e.g., *Trifonov et al*., 1990; *Burtman et al*., 1996]. The Nura main shock shows almost pure reverse faulting on an east striking plane, whereas the aftershocks show both reverse faulting mechanisms similar to the main shock and sinistral strike-slip faulting along northeast trending planes. The thrust earthquakes of the Nura sequence and another reverse-type earthquake along the piedmont of the Pamir in the eastern Alai valley dip rather steep (b in Figures 4a and 6a), 50–70° south, in contrast to the dip of the thrusts at the leading edge of the Pamir thrust system that root in the subhorizontal décollement along the Jurassic evaporites. The Nura earthquake cluster thus highlights the active involvement of the sub-Jurassic basement, well known from the interior of the Pamir thrust system and the Tian Shan. The dips are equal to or steeper than those of the thick-skinned reverse faults, described by *Coutand et al*. [2002] in the western Alai valley.

West of the Nura sequence, along the Trans Alai range south of the Alai valley, microseismicity recedes southward from the leading thrusts (Figure 6). The few thrust earthquakes there occur south of the highest topography and dip ~30° south. However, the majority of the moment tensors along the Trans Alai exhibit dextral strike-slip mechanisms on approximately E(SE) trending planes (Figures 4a and 6). This pattern is confirmed by the centroid moment tensor (CMT) solutions that span 1976–2008 (Figure 6). In fact, the largest instrumentally recorded earthquake on the Pamir's central front southwest of the Alai valley had a strike-slip mechanism, consistent with those determined here (1978 M_w 6.6, Figure 6). A cross section through the central segment of the Pamir thrust system (PTS) (E in Figure 6) shows a subvertical cluster consistent with the strike-slip solutions. The epicenters along the southern margin of the eastern half of the Alai valley form a narrow ESE striking lineament in map view and a very steep south dipping fault in cross section (cross-section F in Figure 6), which is also in agreement with the strike-slip mechanisms, and corresponds to the numerous dextral tear faults mapped in this area (Figure 6). This area is also at the eastern margin of a basement indenter that contains the highest elevations along the Alai range, the Pik Lenin area. The region between this lineament and the thrust front, however, shows little seismicity despite significant north-south convergence being postulated across the thrust system for both long and short timescales [*Strecker et al*., 1995; *Arrowsmith and Strecker*, 1999; *Zubovich et al*., 2010; *Ischuk et al*., 2013].

Further west, where the Alai valley closes and the Tian Shan and the Pamir collide, the Pamir thrust system bends southward. Here earthquakes show thrust mechanisms, with strikes following the oroclinal structure (Figures 3, 4, and 6). The region beneath the Peter I. range is particularly active, with several moderate earthquakes for which we could determine fault plane solutions. The mechanisms in the frontal part of the Peter I. range reflect thrusts with a slight dextral component to mostly dextral slip along steep, ENE striking planes (marked (c) in Figure 4a), following the structural grain. Just behind (south) of these earthquakes, five mechanisms show thrusting on a subhorizontal plane (dip $<10°$), with slip vectors pointing WNW to purely west for the westernmost events (marked (d) in Figure 4a). These earthquakes are very shallow (uppermost 5 km, Figure 2). Southeast of these, a group of three earthquakes are the only strike-slip earthquakes that we may affiliate with the Darvaz fault zone (marked (e) in Figure 4a). Further south, only few earthquakes, too small for focal mechanism determination, testify to activity along the Darvaz fault zone. The faulting pattern of the Peter I. range seems to indicate dextral-transpressive, range-internal deformation,

and westward extrusion of the entire wedge above a subhorizontal décollement between the Vakhsh and Darvaz fault systems. The detachment is likely along the Jurassic evaporites that underlie most of the Tajik-Afghan depression [*Bourgeois et al*., 1997; *Nikolaev*, 2002] and crop out at some of the thrusts in the Peter I. range [*Hamburger et al*., 1992].

At the western margin, near the city of Kulob, where the mountains merge into the Tajik-Afghan basin, we observed more earthquakes with mechanisms exhibiting east-west slip on subhorizontal planes (marked (f) in Figure 4a). We likewise interpret these as movements along the Jurassic décollement. The earthquake depths of ~10 km (Figure 2) agree with the supposed sediment thickness at the eastern margin of the basin [*Nikolaev*, 2002]. This region is known for salt tectonics [*Leith and Simpson*, 1986b], and salt domes pierce the surface close to where the earthquakes are located. Salt normally behaves ductile and hence aseismic at the depth and temperature of the supposed décollement. It is possible, however, that due to diapirism, the salt layer pinches out at places and brings the basement in direct contact with the sediment stack and therefore causes local stick-slip movement. A similar situation occurs beneath the Kohat basin in Pakistan [*Satyabala et al*., 2012]. These earthquakes are valuable because their slip vectors on the detachment give a direct measurement of displacement of the sedimentary stack above the basement, unaffected by internal deformation of the sedimentary rocks. Their pure east-west directions indicate a westward push, and this forcing direction is expressed in the basin's fold trains of parallel westward convex arcs, resembling a top-to-west flow. Within the Tajik-Afghan basin, our event detections are few due to the sparseness of station coverage and the choice of event definition parameters in the detection process [*Sippl et al*., 2013a]. The few available mechanisms are variable and show thrusting, strike-slip, and normal faults. All three normal fault earthquakes are located deeper than 20 km (Figure 2) and hence might be caused by flexing of the basement due to the load of the Pamir [*Schneider et al*., 2013].

5.2. Pamir Interior

Within the Pamir, seismicity roughly forms a cross, centered on a strong earthquake cluster just east of Lake Sarez (Figure 2). The cross-section C in Figure 6 reveals that the cluster has internal structure with several active zones or faults. This shallow cluster also sits on top of a kink in the deep seismic zone (Figure 2). The triangular region of the northeastern Pamir that is enclosed by the two eastern legs of the cross is mostly aseismic, except for some earthquake clusters along the eastern boundary of the Pamir with the Tarim basin. The northeast leg of the cross comprises a lineament, stretching from the Pamir thrust system in the north, across Lake Karakul, to the eastern end of Lake Sarez in the south. Source mechanisms of a few small earthquakes along the lineament are sinistral strike slip. *Strecker et al*. [1995] mapped its surface morphology as en echelon, right-stepping, slightly curved escarpments south of Lake Karakul, with sinistral normal faults also indicated by offset stream channels and fault slip data. Across Lake Karakul, the seismicity bifurcates, with one leg running along the western shore, the other across its center, where an island and a peninsula form a horst (Figures 3 and 6) [*Strecker et al*., 1995; *Amidon and Hynek*, 2010]. The cross-section D in Figure 6 reveals two faults dipping in opposite directions under Lake Karakul, a shallower one reaching depths of about 8 km and dipping east and a deeper one spanning 10–20 km and dipping west. The NNE trending faults can locally be mapped northward, where they interact with the Pamir thrust system. We recorded the most spectacular morphologic expression of the sinistral-oblique normal faulting along the southern Sarez-Karakul fault system, separating the Muskol and Sarez gneiss domes, north of the main earthquake cluster. Here an array of right-stepping, en echelon sinistral-normal fault zones and scarps outline the eastern range front of the Officer's Range (Figure 6). The southeast leg of the cross comprises the Aksu-Murghab and Karasu dextral strike-slip fault zones [*Burtman and Molnar*, 1993; *Strecker et al*., 1995], which connect the dextral Karakorum fault zone with the Sarez-Murghab thrust system (Figures 1 and 3). The seismicity follows this zone only faintly, but two dextral strike-slip earthquakes at the southeastern end of the Aksu-Murghab fault zone are in accordance with its presumed kinematics (marked (g) in Figure 4a).

The two western legs of the "seismic cross" are more diffuse seismic belts (Figure 2). In the southwestern Pamir, seismicity is distributed across the Cenozoic Shakhdara and Alichur gneiss domes. The northwestern termination of this shallow seismic zone coincides with the trend of the intermediate-depth seismic zone (Figure 2). Only in the very west, near the Panj and Shakhdara rivers, earthquakes are big enough to determine their mechanisms. These show sinistral strike-slip deformation on northeast trending (or their conjugate) planes or normal faulting on roughly north-south striking faults (marked (h) in Figure 4a). The

faults related to this cluster can be mapped toward south into the Hindu Kush, where they interact with dextral strike-slip faults that likely form at the eastern tip of the combined Herat-Andarob fault zones [*Stübner et al*., 2013a]. An array of similarly striking faults, with mapable scarps, cuts the Alichur shear zone along the northern margin of the Alichur dome. Another cluster of seismicity farther south across the Wakhan corridor comprises two transtensional mechanisms also on northeast trending or conjugate planes (marked (i) in Figure 4a). This region was quite active during the 1990s, with a series of earthquakes up to M_w 6.1 with normal to transtensional mechanisms in an east-west extension regime (Figure S3). We mapped the related, approximately north striking faults from Wakhan across the South Pamir shear zone of the southern Shakhdara dome. As exhumation along the top-to-SSE normal-slip South Pamir shear zone terminated at 4–2 Ma [*Stübner et al*., 2013b], the current seismicity demonstrates that the deformation field has recently changed from upper crustal approximately NNE-SSW extension to active approximately east-west extension and north-south shortening.

In the western Pamir, a band of earthquakes follows the Vanch range between the Vanch and Yazgulem rivers (profile B in Figure 6) until it turns south around the high mountain massif of the Academy Science Range to reach Lake Sarez (Figures 2, 3, and 6). The earthquakes form several clusters with the strongest being at and south of the confluence of the Vanch and Panj rivers (Figures 3 and 6). This cluster contains an earthquake of M_w 5.3 that caused significant damage in the city of Vanch in January 2010 (marked (j) in Figure 4a and 6a). Mechanisms range from sinistral strike slip on approximately NNE striking or conjugate planes to normal faulting on approximately north trending planes. The earthquakes span a depth range from very shallow to about 10 km depth (profile B in Figure 6). Mapped normal faults occur from north of the Vanch river southward along the Panj river. These faults appear to define an eastern segment of the Badakhshan fault zone, which, however, has a dextral slip sense from offset morphologic features and observation within the fault core in central Badakhshan, Afghanistan. Similar N(N)E trending sinistral strike-slip or conjugate mechanisms occur along the rest of the seismic band. Their ground observation is hindered by the strongly glaciated landscape and the difficult access to this remote area.

6. Discussion

Active tectonics of the Pamir is to a first order prescribed by the northward indentation of the complicated amalgam of the former South Asian margin and the overriding of the basin that once connected the Tajik-Afghan and Tarim basins. Our snapshot of seismicity reveals a pattern of both focused and distributed deformation, indicating both block-like and continuous deformation within the same orogen. This behavior is, as we will show, strongly influenced by Pamir's crustal boundary conditions. The retrieved pattern of seismic deformation is in very good agreement with the surface kinematics revealed by space geodesy.

6.1. Deformation Along the Pamir Front

Seismic deformation of the eastern Pamir is focused at the northern margin, i.e., along the Pamir thrust system. Additional seismicity indicates minor active deformation in the east along the border with the Tarim basin. Compression axes of the double couples for the Nura earthquake cluster in the eastern part of the Pamir thrust system point consistently NNW, i.e., parallel to the GPS velocity vectors in the central and eastern Pamir (Figure 4b). Hence, these earthquakes seem to be an expression of the ~13–15 mm/yr of shortening that GPS measures across the eastern segment of the Pamir thrust system [*Zubovich et al*., 2010; *Ischuk et al*., 2013]. The 1974 M_w 7.0 Markansu earthquake [*Ni*, 1978; *Jackson et al*., 1979; *Burtman and Molnar*, 1993; *Fan et al*., 1994] likewise occurred east of the Alai valley, where the Pamir is colliding with the Tian Shan, and showed a similar reverse mechanism.

In contrast, seismicity is sparser along the central part of the Pamir thrust system, i.e., south of the Alai valley, and no significant thrust earthquake occurred there in the last decades, including our recording period (Figures 4b, 6, and S3). This might either be a sign that the thrust is locked and accumulating elastic strain, as is postulated for the Main Himalaya Thrust [*Ader et al*., 2012], or that it is creeping. Scarps and a series of apparently synchronal rockslides, however, indicate that the frontal thrust is capable of producing large earthquakes [*Nikonov*, 1988; *Strecker et al*., 1995; *Arrowsmith and Strecker*, 1999]. At right angle to the ~13–15 mm/yr approximately north-south shortening across the Pamir thrust system, there is also a ~5 mm/yr westward motion measured with GPS [*Zubovich et al*., 2010, Figure 7] that implies dextral slip along the approximately east trend of the Pamir thrust system. Our finding of W(NW) trending dextral strike-slip

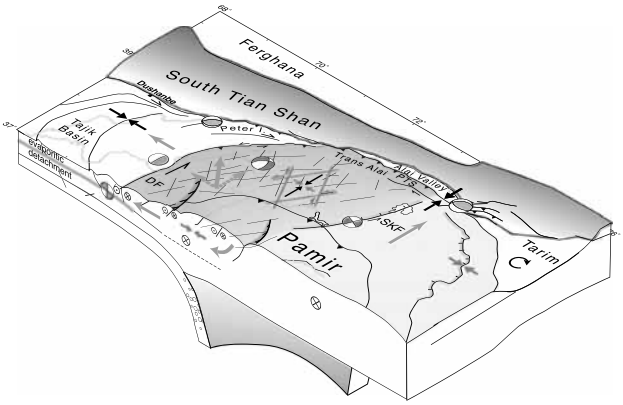

Figure 7. Interpretational block diagram showing the stresses (black = σ_1 and red = σ_3 directions), type of faulting, and resulting kinematics (green arrows) of the Pamir. The eastern Pamir is pushed north en bloc, where it causes shortening at its northern perimeter (PTS = Pamir thrust system). The western Pamir is also pushed north but at the same time deforms internally by strike-slip faulting under north-south compression and by normal faulting producing east-west extension, overall causing westward extrusion and north-south shortening. The westward extrusion causes shortening of the Tajik-Afghan basin sediments above an evaporitic décollement. The observed seismic faulting pattern explains the anticlockwise rotation of GPS velocity vectors observed across the Pamir from east to west. DF = Darvaz fault system; SKF = Sarez-Karakul fault system.

earthquakes south of the leading edge of the Pamir thrust system might point to present-day slip partitioning in frontal thrusting and more internal lateral escape. Except for the Nura earthquake and its aftershocks, it appears that we have observed only the strike-slip part of the partitioned system during our observation period in the Trans Alai range south of the Alai valley. The seismic cross-sections E and F in Figure 6 through active strike-slip faults show that the events are aligned subvertically over a depth range of ~2–12 km. Layer thickness above the Jurassic salt décollement is only 3.5 km in the eastern and ~5.5 km in the western Alai valley [*Vlasov et al*., 1991; *Coutand et al*., 2002]. Hence, if the faults imaged here and possibly of the entire Pamir thrust system root in a common décollement, it must be below the Jurassic evaporites.

6.2. Deformation in the Pamir Interior

The lack of both thrusting and significant seismicity in the eastern Pamir's interior demonstrates that it is moving northward *en bloc*; this is in agreement with the GPS data (Figure 4b). We attribute the seismicity in the Chinese Pamir to the Muji graben and Kongur Shan normal fault zone and farther east, to thrusting of the Chinese Pamir over the Tarim basin (Figure 3). As our seismic network lacked stations in the Chinese Pamir for most of the recording time, our catalog for this region may be incomplete, i.e., we might underestimate the true rate of seismicity there. The Kongur Shan normal fault system has accommodated ≥35 km of east-west extension, mostly since ~7 Ma [*Brunel et al*., 1994; *Robinson et al*., 2004, 2007; *Thiede et al*., 2013]. This extension has been attributed to gravitational collapse or radial spreading [*Brunel et al*., 1994; *Strecker et al*., 1995], thermal and gravitational effects of a lithospheric tear fault [*Thiede et al*., 2013], or linked to the extension system in southwestern Tibet via the Karakorum fault zone [*Ratschbacher et al*., 1994]. Local extension is ongoing, as implied by the divergence of the GPS velocity field between the Pamir's interior and Tarim block (Figure 4b), which might simply be attributed to the clockwise rotation of a rigid Tarim block (Figure 7) [*Avouac et al*., 1993; *Reigber et al*., 2001], in agreement with the southward decrease of extension along the Muji-Kongur Shan graben system [*Robinson et al*., 2004].

Within the Pamir, the Sarez-Karakul fault system separates the mostly undeformed high plateau of the eastern Pamir from the seismically active, high-relief, and deeply incised western Pamir. The fault system accommodates sinistral shear and approximately east-west extension between these two regions (Figures 3 and 6). The Karakul graben shows subdued geomorphic imprint with probably only a few kilometers of east-west extension [*Strecker et al*., 1995]. West of the Officer's Range (Figure 6a), however, the spectacular sinistral-oblique normal faults with clear surface breaks and major topographic differences (Figures 6b and 6c) imply comparably frequent and large neotectonic activity. The Sarez-Karakul fault system can be traced by an array of distributed and discontinuous faults across Lake Sarez and farther south into the Alichur and Shakhdara domes. Here the normal and sinistral strike-slip deformation involves much less displacement.

The large M ~7.7 1911 Sarez earthquake blocked the Murghab River by a giant rockfall, creating Earth's highest dam (Usoi "landslide" dam) and Lake Sarez, still up to 550 m deep [*Galitzin*, 1915; *Jeffreys*, 1923; *Schuster and Alford*, 2004; *Ischuk*, 2011]. Based on historic accounts of intensity, *Ambraseys and Bilham* [2012] and *Bindi et al*. [2013] placed the epicenter somewhere at the western end of Lake Sarez (Figure 6). It was

by far the largest earthquake to have occurred in the Pamir crust in historic time. An earthquake of this size needs a fault that allows a more or less unimpeded rupture of about 120–170 km length, depending on the fault type [e.g., *Blaser et al*., 2010]. The only seismically active structure of this dimension near the assumed epicenter seems to be the Sarez-Karakul fault system, which also shows a series of neotectonic structures along its trace. Although the isoseismal contours are more elongated east-west in the *Ambraseys and Bilham* [2012] model, they might be biased due to a lack of observations in the central Pamir. This region was practically uninhabited during winter when the Sarez earthquake occurred. Alternatively, the Sarez-Murghab thrust system and its eastward connection into the Aksu-Murghab fault zone may have been the locus of the Sarez earthquake. We observed dextral-oblique thrusts with unconsolidated cataclasite in the upper Bartang valley west of the Lake Sarez, pulverized fault gouge in imbricated Cretaceous granite (Figure 6d), and ultracataclasite along faults that stack granite and possibly Tertiary clastic rocks at Lake Sarez (Figure 6e). A relief with all slopes at the angle of response and with erosion dominated by rockfalls and landslides prevents easy identification of scarps. We mapped scarps ~50 km east of Lake Sarez along the westernmost strands of the Aksu-Murghab fault zone, in the accessible part of the upper Murghab River. Massive rockfalls also accommodate possibly active faults in the core of the Sarez dome north of Lake Sarez. The current aseismicity of the Sarez-Murghab thrust system may reflect stress relaxation after the large Sarez earthquake. However, a definite localization of this event must await a reexamination of the existing historical seismograms and a more detailed mapping of surface scarps, especially in the high-altitude area south of Lake Sarez (Figure 3).

West of the Sarez-Karakul fault system and in the southwestern Pamir, a high rate of distributed crustal seismicity implies active deformation. Source mechanisms exhibit mainly sinistral strike-slip faulting on northeast striking or conjugate planes or normal faulting on north striking planes, indicating north-south compression and east-west extension (Figures 4b and 6a). The prevalence of strike-slip faults within the Pamir indicates that σ_3, the least compressive stress, is horizontal and points east-west (Figures 4b and 7). We suggest that the Tajik-Afghan basin, with its ≤10 km of sedimentary rocks above a ductile décollement, constitutes an essentially open lateral boundary, exerting minimal resistance to westward extrusion of at least the western Pamir upper crust. *Stübner et al*. [2013a, 2013b] suggested a similar scenario of collapse of the upper ~35 km of crust in the giant Shakhdara dome at the western margin of the Pamir Plateau into the Tajik-Afghan basin, based on the compatibility in the kinematics and amount of strain (extension in the gneiss dome and shortening across the basin), timing of extension and shortening (Miocene and Pliocene), and the likely presence of low viscosity, partially molten crust starting at ~15 km depth beneath the southern Pamir Plateau [*Sippl et al*., 2013b; *Stearns et al*., 2013; *Sass et al*., 2014; see below]. Our seismic record and the GPS data show that this process is ongoing and has prograded northward, incorporating the entire western Pamir, albeit with diminished rates and a change of σ_1 from vertical in the Miocene-Pliocene (during the formation of the Shakhdara dome) to subhorizontal at present.

Knowledge about active deformation features in the high-relief western Pamir is scarce. Whereas approximately north trending faults were mapped in the southwestern Pamir (across the Shakhdara and Alichur domes), we were unable to identify more than a few active features north of the Sarez-Murghab and west of the Sarez-Karakul fault zones (Figure 3). This may be because the western Pamir Yazgulem and Academy of Science Ranges contain the highest topography and most widespread glaciation and thus the most youthful morphology and most difficult accessibility of the entire Pamir. Alternatively or additionally, the relative low magnitude and distributed nature of crustal seismicity, together with possible youthfulness of the present-day stress field in this area, may not yet have established its distinct fault pattern, recognizable as mapable fault arrays. We note, however, that significant numbers of glacier-filled valleys in the central western Pamir trend NNE (Figure 3), subparallel to the possibly active nodal planes of our strike-slip solutions. Similarly, *Fuchs et al*. [2013] argued that active tectonics plays a role in controlling the Panj, i.e., the trunk river draining the Pamir (Figure 3). Our results at least support that the NNE flowing segments of the Panj are parallel to the active sinistral-normal faults of the western Pamir.

The southwestern Pamir Shakhdara dome was exhumed under approximately NNW-SSE extension until 4–2 Ma and coevally and in opposition to bulk north-south shortening [*Stübner et al*., 2013a, 2013b], i.e., at a relative high angle to the current approximately east-west tension. The dome also leaves its thermal imprint as a prominent low-velocity zone at midcrustal level in seismic tomography (Figure S1) [*Sippl et al*., 2013b] and magnetotelluric imaging [*Sass et al*., 2014], corroborating the relatively young exhumation age. If

we assume that both flow in the ductile crust observed in the Shakhdara dome and brittle fault slip observed in earthquakes react to the ambient stress regime, this implies a recent rotation of the stress regime. This rotation might have been induced by the commencing collision of the Pamir with the Tian Shan, which inhibited further expansion of the Pamir Plateau toward the north. The concurrent occurrence of strike-slip and normal faulting within the Pamir indicates that the maximum horizontal (north-south) and vertical compressive stresses are similar in magnitude and hence that the plateau will not be able to sustain much more thickening. The generally north or northeast trending active faults in the Pamir are not congruent with the majority of the Cenozoic east-west structures. This is a further indication that the current deformation regime is young and has not left a strong imprint in the structural grain.

6.3. Westward Extrusion of the Western Pamir Into the Tajik-Afghan Depression

GPS velocity vectors change anticlockwise from NNW in the eastern Pamir to WNW within the Tajik-Afghan depression (Figure 4b). This rotation may be explained by the superposition of two principal components of motion that are oriented perpendicular to one another, namely, the bulk northward movement due to the tectonic forces of the northward push and the westward component driven by the gravitational forces from the topographic contrast between the ~4 km high plateau and the ~0.5 km high Tajik-Afghan depression. The GPS measurements are not dense enough to locate where east-west extension in the western Pamir sets in. We suggest that it is where seismic deformation starts, i.e., along the Sarez-Karakul fault system (Figure 7).

While westward extrusion of the Pamir might involve the whole crust [*England and McKenzie*, 1982], its accommodation in the Tajik-Afghan basin is probably different below and above the detachment level. The sedimentary rocks are shortened in a thin-skinned mode above a layer of Jurassic evaporite [*Nikolaev*, 2002] that decouples them from the underlying basement. The Cenozoic thrusts and folds constitute a series of westward convex arcs, indicating a westward directed compressional force. The basement beneath the deforming sediments seems to be downward flexed by the western Pamir, probably without much internal shortening [*Sippl et al*., 2013b]. The GPS measurements show that the total amount of the approximately east-west shortening across the Tajik-Afghan basin roughly equals the total amount of extension across the Pamir [*Ischuk et al*., 2013]; hence, no net convergence between the basin and the Pamir is required. The mantle lithosphere and possibly lower crust beneath the Tajik-Afghan basin, however, dip southeast to east to depths of at least 250 km beneath the Pamir (Figures 1, 2, and 7), as indicated by the active Wadati-Benioff zone and lithospheric imaging [*Schneider et al*., 2013; *Sippl et al*., 2013a, 2013b]. If there is little or no east-west convergence below the detachment level, the Pamir slab geometry cannot be explained by subduction alone but must involve other geodynamic processes, e.g., delamination. While the western Pamir thrusts over the Tajik-Afghan basin, it is also moving northward relative to the basin at about 10 mm/yr, measured by GPS. Generally, this shear is attributed to the Darvaz fault, which shows sinistral offset features with the few dated features confirming a rate in this order of magnitude [*Trifonov*, 1978].

6.4. Crustal Boundary Conditions Versus Influence of Deep Processes

The Pamir features, quite uniquely, vigorous intermediate-depth seismicity that accompanies a descending lithospheric plate into the mantle to depth >250 km. It is interesting to see how such a deep-seated process affects the short timescale deformation of the shallow crust observed in crustal earthquakes and surface strain from GPS measurements and the longer-term tectonics from Cenozoic structures. The intermediate-depth seismicity beneath the Pamir forms a tight 90° arc that reaches deepest at its southwestern end, where it dips steeply east to depths of ~250 km (Figure 2) [*Sippl et al*., 2013a]. *Schneider et al*. [2013] showed that these earthquakes occur in an ~11 km thick low-velocity zone that could be traced all the way to the Moho of the northern Pamir. Together with the results of a local earthquake tomography [*Sippl et al*., 2013b], it seems that under the eastern Pamir the cold Asian mantle lithosphere descends together with the lower crust and a part of the overlying middle crust. At ~90–100 km depth, the middle crust detaches, and only the lower crust and mantle sink to greater depths, whereas the middle and upper crusts contribute to crustal thickening. *Sobel et al*. [2013] attributed the tight curvature of the Pamir slab to rollback of a curved plate, subducting southward along the Pamir thrust system, while tearing away from the Tarim basin crust in the east along a northward propagating subduction-transform edge fault [*Govers and Wortel*, 2005]. In such a scenario, however, the subducted slab should reach deepest in north-south direction, which is not the case when taking the seismicity as a proxy for the plate. A rollback of an outward propagating subduction arc should produce north-south and northwest-southeast extension in its upper plate [*Heuret and*

Lallemand, 2005]. Although this is in gross agreement with the Cenozoic structures, e.g., the extensional gneiss domes of the Pamir (Figure 3), it does not reflect the recent stress field observed in the crustal earthquakes. Alternatively, *Sippl et al*. [2013a] noted that delamination of mantle lithosphere and lower crust could produce a similar geometry as observed today. Delamination produces shortening above the delaminating hinge and extension above the resulting lithospheric gap due to asthenospheric inflow that heats the crust above [*Göğüş and Pysklywec*, 2008]. However, in the case of the India-Asia collision, the lithospheric gap is likely quickly closed by the Indian indenter [*Sippl et al*., 2013b].

The large-scale tectonic forces and the crustal boundary conditions (Figure 7) may more straightforwardly explain our observations of the shallow crustal deformation field in the Pamir. Driven by the tectonic force exerted by the indentation of India, the Pamir moves northward in its entirety, which is largely accommodated by thrusting along its northern margin and strike-slip faulting along its flanks. The significant topography created by shortening and uplift of the Pamir (average elevation of the Pamir Plateau is ~4 km) causes gravitational forces that try to spread and lower the topography. Toward the north, this is blocked by the collision with the Tian Shan. In the east, the strong, cratonic Tarim crust itself has quite high elevation of >2 km and might also act as a barrier for Pamir crust to spread. Some extension between the Pamir and Tarim may be caused by Tarim's clockwise rotation relative to the Pamir (Figure 7). The Tajik-Afghan depression in the west opens the easiest way for Pamir rocks to extrude and also has the largest topographic contrast to the Pamir Plateau.

Speculatively, the distinctly different seismicity in the western and eastern Pamir and in particular the recent development of the Sarez-Karakul fault system and its distributed continuation across the southwestern Pamir into the Hindu Kush of Afghanistan may have an additional, superregional cause (Figure 1). It may reflect that the western transform margin at India's western margin is progressively propagating northeastward, from the Chaman fault system, displaced by the Andarab and Herat faults system, overstepping the Tirich Mir and Reshun fault systems, into the Pamir. The Sarez-Karakul fault system may start to link up, along the sinistral fault systems south of the Talas-Fergana fault, with the Tian Shan east of the Talas-Fergana system, which, from its bulk orientation to the India-Asia collision, carries a sinistral strike-slip component [*Cobbold and Davy*, 1988; *Cobbold et al*., 1994; *Houseman and England*, 1996]. Extrapolating this scenario to the lithospheric scale would also suggest that the sigmoidal shape of the active intracontinental plate boundary, traced by the depth contours of deep seismicity and incorporating along-strike slab tears (Figures 1 and 2), merely reflects delamination of Asian lithosphere and filling of the created space by the northeastward progression of India's western promontory.

7. Conclusions

We used 2 years of seismicity data and earthquake source mechanisms from local seismic networks to characterize the current crustal deformation of the Pamir and its surroundings. It appears that the Pamir east of a lineament between lakes Sarez and Karakul moves northward en bloc, with little internal deformation. At the northern boundary of this trapezoidal region, the Pamir collides with the Tian Shan and high seismicity along this frontal Pamir thrust system reflects focused shortening. The NNE striking Sarez-Karakul fault system and its southwestward continuation into the Hindu Kush of Afghanistan by more distributed deformation indicate sinistral shear and east-west extension between the eastern and the western Pamir. The western Pamir shows higher seismic deformation rates dominated by sinistral strike-slip faulting on northeast trending or conjugate planes and normal faulting, indicating overall east-west extension and some north-south shortening. We explain this deformation pattern by ongoing collapse of the western margin of the Pamir Plateau and westward extrusion of Pamir rocks into the Tajik-Afghan depression. Here it causes thin-skinned shortening of Tajik-Afghan basin rocks above a weak evaporitic décollement. Surprisingly, this westward motion also dominates the central part of the Pamir thrust system at the northern edge of the Pamir, as indicated by dextral strike-slip faulting along the Trans Alai range despite the significant north-south shortening predicted by GPS measurements. However, this might be due to the short observation period, during which only one part of a partitioned slip system is seismically active.

Superposition of Pamir's bulk northward movement and collapse and westward extrusion of its western flank causes gradual rotation of surface velocities from NNW to WNW, as observed by GPS measurements. This pattern can, to the first order, be explained by the local boundary conditions, i.e., the collision of the

Pamir with the Tian Shan in the north, the rheologically strong Tarim block and its clockwise rotation in the east, and the Tajik-Afghan basin in the west, with its weak sedimentary rocks above a evaporitic décollement and a downward flexed and possibly delaminating mantle and lower crust, which represent an open boundary for the Pamir rocks to extrude. The overall pattern may, however, be driven by the long-term geodynamic processes along the western edge of the India-Asia collision. It appears that the distinctly different seismicity in the western and eastern Pamir and in particular the development of the Sarez-Karakul fault system and its distributed continuation across the southwestern Pamir into the Hindu Kush of Afghanistan may reflect the continuous propagation of the western transform margin of the orogen toward northeast. The push and topographic load of India and that of the Asian blocks that were accreted to India during the northward progradation of the intracontinental deformation may progressively delaminate Asian lithosphere during its advance with a northward propagating delamination front at the western margin of the orogen. Thus, two major players, the prograding western edge of the collision and the ensuing crustal thickness gradient between the orogen and its lateral foreland, may be responsible for the complex 3-D pattern of the Pamir deformation field. It remains a major challenge to trace this evolution throughout the ~50 Myr development of the India-Asia collision.

Acknowledgments
This research was funded by DFG bundle TIPAGE (PAK 443), the CAME project bundle TIPTIMON, funded by the German Federal Ministry of Education and Research (support code 03G0809), and GFZ. Seismic instruments for the FERGHANA and TIPAGE networks were provided by the Geophysical Instrument Pool Potsdam (GIPP). Work in Tajikistan and Afghanistan would have been impossible without the continuous support of the Tajik Academy of Sciences, in particular M.I. Ilolov, and Focus Humanitarian Assistance, an affiliate of the Aga Khan Development Network. We thank the entire TIPAGE group for joint fieldwork, discussions, and support. Konstanze Stübner donated the photo of Figure 6b originating form joint fieldwork. We thank Rebecca Bendick and an anonymous referee for very useful comments that improved the manuscript. Source parameters derived in this study are available as Tables S1 and S2 in the supporting information.

References

Ader, T., et al. (2012), Convergence rate across the Nepal Himalaya and interseismic coupling on the Main Himalayan Thrust: Implications for seismic hazard, *J. Geophys. Res.*, *117*, B04403, doi:10.1029/2011JB009071.

Ambraseys, N., and R. Bilham (2012), The Sarez-Pamir earthquake and landslide, *Seismol. Res. Lett.*, *83*(2), 294–314, doi:10.1785/gssrl.83.2.294.

Amidon, W. H., and S. A. Hynek (2010), Exhumational history of the north central Pamir, *Tectonics*, *29*, TC5015, doi:10.1029/2009TC002589.

Arrowsmith, J. R., and M. R. Strecker (1999), Seismotectonic range-front segmentation and mountain-belt growth in the Pamir-Alai region, Kyrgyzstan (India-Eurasia collision zone), *Geol. Soc. Am. Bull.*, *111*(11), 1665–1683, doi:10.1130/0016-7606(1999).

Avouac, J. P., P. Tapponnier, M. Bai, H. You, and G. Wang (1993), Active thrusting and folding along the northern Tien Shan and Late Cenozoic rotation of the Tarim relative to Dzungaria and Kazakhstan, *J. Geophys. Res.*, *98*, 6755–6804, doi:10.1029/92JB01963.

Beaumont, C., R. A. Jamieson, M. H. Nguyen, and B. Lee (2001), Himalayan tectonics explained by extrusion of a low-viscosity crustal channel coupled to focused surface denudation, *Nature*, *414*(6865), 738–742, doi:10.1038/414738a.

Billington, S., B. L. Isacks, and M. Barazangi (1977), Spatial distribution and focal mechanisms of mantle earthquakes in the Hindu Kush-Pamir region: A contorted Benioff zone, *Geology*, *5*(11), 699–704.

Bindi, D., S. Parolai, A. Gómez-Capera, M. Locati, Z. Kalmetyeva, and N. Mikhailova (2013), Locations and magnitudes of earthquakes in Central Asia from seismic intensity data, *J. Seismol.*, *18*(1), 1–21, doi:10.1007/s10950-013-9392-1.

Bird, P. (1979), Continental delamination and the Colorado Plateau, *J. Geophys. Res.*, *84*, 7561–7571, doi:10.1029/JB084iB13p07561.

Blaser, L., F. Krüger, M. Ohrnberger, and F. Scherbaum (2010), Scaling relations of earthquake source parameter estimates with special focus on subduction environment, *Bull. Seismol. Soc. Am.*, *100*(6), 2914–2926, doi:10.1785/0120100111.

Bourgeois, O., P. R. Cobbold, D. Rouby, J.-C. Thomas, and V. Shein (1997), Least squares restoration of Tertiary thrust sheets in map view, Tajik depression, central Asia, *J. Geophys. Res.*, *102*(B12), 27,553–27,573, doi:10.1029/97JB02477.

Brunel, M., N. Arnaud, P. Tapponnier, Y. Pan, and Y. Wang (1994), Kongur Shan normal fault: Type example of mountain building assisted by extension (Karakoram fault, eastern Pamir), *Geology*, *22*, 707–710.

Burtman, V. S., and P. Molnar (1993), *Geological and Geophysical Evidence for Deep Subduction of Continental Crust Beneath the Pamir*, *Geol. Soc. Am. Spec. Pap.*, *281*, 76 pp.

Burtman, V. S., S. F. Skobelev, and P. Molnar (1996), Late Cenozoic slip on the Talas-Ferghana fault, the Tien Shan, central Asia, *Geol. Soc. Am. Bull.*, *108*(8), 1004–1021, doi:10.1130/0016-7606(1996)108.

Cobbold, P. R., and P. Davy (1988), Intendation tectonics in nature and experiment. 2. Central Asia, *Bull. Geol. Inst., Univ. Uppsala, New Ser.*, *14*, 143–162.

Cobbold, P. R., E. Sadybakasov, and J. C. Thomas (1994), Cenozoic transpression and basin development, Kyrgyz Tien Shan, Central Asia, in *Geodynamic Evolution of Sedimentary Basins*, edited by F. Roure et al., pp. 181–202, International Symposium, Moscow.

Copley, A., J. P. Avouac, and B. P. Wernicke (2011), Evidence for mechanical coupling and strong Indian lower crust beneath southern Tibet, *Nature*, *472*(7341), 79–81, doi:10.1038/nature09926.

Coutand, I., M. R. Strecker, J. R. Arrowsmith, G. E. Hilley, R. C. Thiede, A. Korjenkov, and M. Omuraliev (2002), Late Cenozoic tectonic development of the intramontane Alai Valley, (Pamir-Tien Shan region, central Asia): An example of intracontinental deformation due to the Indo-Eurasia collision, *Tectonics*, *21*(6), 1053, doi:10.1029/2002TC001358.

Cowgill, E. (2010), Cenozoic right-slip faulting along the eastern margin of the Pamir salient, northwestern China, *Geol. Soc. Am. Bull.*, *122*(1–2), 145–161, doi:10.1130/B26520.1.

Dewey, J. F. (1988), Extensional collapse of orogens, *Tectonics*, *7*, 1123–1139, doi:10.1029/TC007i006p01123.

Doebrich, J. L., and R. R. Wahl (Compilators) (2006), Geological and mineral resource map of Afghanistan: Version 2, *U.S. Geol. Surv. Open File Rep., 2006–1038*.

Dziewonski, A., T.-A. Chou, and J. H. Woodhouse (1981), Determination of earthquake source parameters from waveform data for studies of global and regional seismicity, *J. Geophys. Res.*, *86*, 2825–2852, doi:10.1029/JB086iB04p02825.

Ekström, G., M. Nettles, and A. Dziewoński (2012), The global CMT project 2004–2010: Centroid-moment tensors for 13,017 earthquakes, *Phys. Earth Planet. Inter.*, *2000*, 1–9, doi:10.1016/j.pepi.2012.04.002.

England, P., and D. McKenzie (1982), A thin viscous sheet model for continental deformation, *Geophys. J. R. Astron. Soc.*, *70*, 295–321.

Evans, S. G., N. J. Roberts, A. Ischuk, K. B. Delaney, G. S. Morozova, and O. Tutubalina (2009), Landslides triggered by the 1949 Khait earthquake, Tajikistan, and associated loss of life, *Eng. Geol.*, *109*(3–4), 195–212, doi:10.1016/j.enggeo.2009.08.007.

Fan, G., J. F. Ni, and T. Wallace (1994), Active tectonics of the Pamirs and Karakorum, *J. Geophys. Res.*, *99*(B4), 7131–7160, doi:10.1029/93JB02970.
Flesch, L., and R. Bendick (2012), The relationship between surface kinematics and deformation of the whole lithosphere, *Geology*, *40*(8), 711–714, doi:10.1130/G33269.1.
Flesch, L. M., W. E. Holt, P. G. Silver, M. Stephenson, C.-Y. Wang, and W. W. Chan (2005), Constraining the extent of crust-mantle coupling in central Asia using GPS, geologic, and shear wave splitting data, *Earth Planet. Sci. Lett.*, *238*, 248–268, doi:10.1016/j.epsl.205.06.023.
Fu, B., Y. Ninomiya, and J. Guo (2010), Slip partitioning in the northeast Pamir-Tian Shan convergence zone, *Tectonophysics*, *483*, 344–364, doi:10.1016/j.Tect0.2009.11.003.
Fuchs, M. C., R. Gloaguen, and E. Pohl (2013), Tectonic and climatic forcing on the Panj river system during the Quaternary, *Int. J. Earth Sci.*, *102*(7), 1985–2003, doi:10.1007/s00531-013-0916-2.
Galitzin, B. (1915), Sur le tremblement de terre du 18 fevrier 1911, *Comptes Rendues*, *160*, 810–813.
Göğüş, O. H., and R. N. Pysklywec (2008), Near-surface diagnostics of dripping or delaminating lithosphere, *J. Geophys. Res.*, *113*(B11), 1–11, doi:10.1029/2007JB005123.
Govers, R., and M. J. R. Wortel (2005), Lithosphere tearing at STEP faults: Response to edges of subduction zones, *Earth Planet. Sci. Lett.*, *236*(1–2), 505–523, doi:10.1016/j.epsl.2005.03.022.
Haberland, C., U. Abdybachaev, B. Schurr, H. U. Wetzel, S. Roessner, A. Sarnagoev, S. Orunbaev, and C. Janssen (2011), Landslides in southern Kyrgyzstan: Understanding tectonic controls, *Eos Trans. AGU*, *92*(20), 169–176, doi:10.1029/2011EO200001.
Hamburger, M. W., D. R. Sarewitz, T. L. Pavlis, and G. A. Popandopulo (1992), Structural and seismic evidence for intracontinental subduction in the Peter the First Range, Central Asia, *Geol. Soc. Am. Bull.*, *104*(4), 397–408, doi:10.1130/0016-7606(1992).
Hardebeck, J. L., and P. M. Shearer (2002), A new method for determining first-motion focal mechanisms, *Bull. Seismol. Soc. Am.*, *92*(6), 2264–2276.
Heuret, A., and S. Lallemand (2005), Plate motions, slab dynamics and back-arc deformation, *Phys. Earth Planet. Inter.*, *149*(1–2), 31–51, doi:10.1016/j.pepi.2004.08.022.
Houseman, G., and P. England (1996), A lithospheric-thickening model for the Indo-Asian collision, in *The Tectonic Evolution of Asia*, edited by A. Yin and T. M. Harrison, pp. 1–17, Cambridge Univ. Press, Cambridge, U. K.
Ischuk, A. (2011), Usoi rockslide dam and Lake Sarez, Pamir Mountains, Tajikistan, in *Natural and Artificial Rockslide Dams*, *Lect. Notes Earth Sci.*, vol. 133, edited by S. G. Evans et al., pp. 423–440.
Ischuk, A., et al. (2013), Kinematics of the Pamir and Hindu Kush regions from GPS geodesy, *J. Geophys. Res. Solid Earth*, *118*, 2408–2416, doi:10.1002/jgrb.50185.
Jackson, J., P. Molnar, H. Patton, and T. Fitch (1979), Seismotectonic aspects of the Markansu valley, Tadjikstan, earthquake of August 11, 1974, *J. Geophys. Res.*, *84*(B11), 6157–6167, doi:10.1029/JB084iB11p06157.
Jeffreys, H. (1923), The Pamir earthquake of 1911 February 18, in relation to the depths of earthquake foci, *Monthly Notes Royal Astr. Soc. Geophys. Suppl.*, *1*, 22–31.
Krumbiegel, C., B. Schurr, S. Orunbaev, H. Rui, and L. Pingren (2011), The 05/10/2008 Mw 6.7 Nura earthquake sequence on the main Pamir Thrust, *Geophys. Res. Abstr.*, *13*, EGU2011-4846.
Leith, W., and D. W. Simpson (1986a), Seismic domains within the Gissar-Kokshal seismic zone, Soviet Central Asia, *J. Geophys. Res.*, *91*, 689–699, doi:10.1029/JB091iB01p00689.
Leith, W., and D. W. Simpson (1986b), Earthquakes related to active salt doming near Kulyab, Tadjikistan, USSR, *Geophys. Res. Lett.*, *13*(10), 1019–1022, doi:10.1029/GL013i010p01019.
Li, T., J. Chen, J. A. Thompson, D. W. Burbank, and W. Xiao (2012), Equivalency of geologic and geodetic rates in contractional orogens: New insights from the Pamir Frontal Thrust, *Geophys. Res. Lett.*, *39*, LI5305, doi:10.1029/2012GL051782.
Lukk, A. A., S. L. Yunga, V. I. Shevchenko, and M. W. Hamburger (1995), Earthquake focal mechanisms, deformation state and seismotectonics of the Pamir-Tien Shan region, Central Asia, *J. Geophys. Res.*, *100*(B10), 20,321–20,343, doi:10.1029/95JB02158.
Mechie, J. X., et al. (2012), Crustal and uppermost mantle velocity structure along a profile across the Pamir and southern Tien Shan as derived from project TIPAGE wide-angle seismic data, *Geophys. J. Int.*, *188*, 385–407, doi:10.1111/j.1365-246X.2011.05278.x.
Mohadjer, S., et al. (2010), Partitioning of India-Eurasia convergence in the Pamir-Hindu Kush from GPS measurements, *Geophys. Res. Lett.*, *37*, L04305, doi:10.1029/2009GL041737.
Ni, J. F. (1978), Contemporary tectonics in the Tien Shan region, *Earth Planet. Sci. Lett.*, *41*(3), 347–354.
Nikolaev, V. G. (2002), Afghan-Tajik depression: Architecture of sedimentary cover and evolution, *Russ. J. Earth Sci.*, *4*(6), 399–421.
Nikonov, A. (1988), Reconstruction of the main parameters of old large earthquakes in Soviet Central Asia using the paleoseismogeological method, *Tectonophysics*, *147*(3–4), 297–312, doi:10.1016/0040-1951(88)90191-6.
Pavlis, T. L., M. W. Hamburger, and G. L. Pavlis (1997), Erosional processes as a control on the structural evolution of an actively deforming fold and thrust belt: An example from the Pamir-Tien Shan region, central Asia, *Tectonics*, *16*(5), 810–822, doi:10.1029/97TC01414.
Pegler, G., and S. Das (1998), An enhanced image of the Pamir-Hindu Kush seismic zone from relocated earthquake hypocentres, *Geophys. J. Int.*, *134*(2), 573–595, doi:10.1046/j.1365-246x.1998.00582.x.
Ratschbacher, L., O. Merle, P. Davy, and P. Cobbold (1991), Lateral extrusion in the Eastern Alps, Part 1: Boundary conditions and experiments scaled for gravity, *Tectonics*, *10*(2), 245–256, doi:10.1029/90TC02622.
Ratschbacher, L., W. Frisch, G. Liu, and C. Chen (1994), Distributed deformation in southern and western Tibet during and after the India-Asia collision, *J. Geophys. Res.*, *99*, 19,917–19,945, doi:10.1029/94JB00932.
Reigber, C., G. W. Michel, R. Galas, D. Angermann, J. Klotz, J. Y. Chen, A. Papschev, R. Arslanov, V. E. Tzurkov, and M. C. Ishanov (2001), New space geodetic constraints on the distribution of deformation in Central Asia, *Earth Planet. Sci. Lett.*, *191*(1–2), 157–165, doi:10.1016/S0012-821X(01)00414-9.
Robinson, A. C., A. Yin, C. E. Manning, T. M. Harrison, S.-H. Zhang, and X.-F. Wang (2004), Tectonic evolution of the northeastern Pamir: Constraints from the northern portion of the Cenozoic Kongur Shan extensional system, western China, *Geol. Soc. Am. Bull.*, *116*(7/8), 953–973, doi:10.1130/B25375.1.
Robinson, A. C., A. Yin, C. E. Manning, T. M. Harrison, S.-H. Zhang, and X.-F. Wang (2007), Cenozoic evolution of the eastern Pamir: Implications for strain-accommodation mechanisms at the western end of the Himalayan-Tibetan orogen, *Geol. Soc. Am. Bull.*, *119*(7/8), 882–896, doi:10.1130/B25981.1.
Rutte, D., M. Stearns, and L. Ratschbacher (2013), The eastern Central Pamir Gneiss Domes: Temporal and spatial geometry of burial and exhumation, *Geophys. Res. Abstr.*, *15*, EGU2013-6090-2.
Sass, P., O. Ritter, L. Ratschbacher, V. A. Matiukov, A. K. Rybin, and V. Y. Batalev (2014), Resistivity structure underneath the Pamir and Southern Tian Shan, *Geophys. J. Int.*, doi:10.1093/gji/ggu146.

Satyabala, S. P., Z. Yang, and R. Bilham (2012), Stick-slip advance of the Kohat Plateau in Pakistan, *Nat. Geosci.*, *5*, 147–150, doi:10.1038/NGEO1373.

Schmidt, J., B. R. Hacker, L. Ratschbacher, K. Stübner, M. Stearns, A. Kylander-Clark, J. M. Cottle, A. A. G. Webb, G. Gehrels, and V. Minaev (2011), Cenozoic deep crust in the Pamir, *Earth Planet. Sci. Lett.*, *312*(3–4), 411–421, doi:10.1016/j.epsl.2011.10.034.

Schneider, F. M., et al. (2013), Seismic imaging of subducting continental lower crust beneath the Pamir, *Earth Planet. Sci. Lett.*, *375*, 101–112, doi:10.1016/j.epsl.2013.05.015.

Schurr, B., and J. Nábělek (1999), New techniques for the analysis of earthquake sources from local array data with an application to the 1993 Scotts Mills, Oregon, aftershock sequence, *Geophys. J. Int.*, *137*(3), 585–600, doi:10.1046/j.1365-246x.1999.00771.x.

Schuster, R. L., and D. Alford (2004), Usoi landslide dam and Lake Sarez, Pamir Mountains, Tajikistan, *Environ. Eng. Geosci.*, *10*(2), 151–168.

Schwab, M., et al. (2004), Assembly of the Pamirs: Age and origin of magmatic belts from the southern Tien Shan to the southern Pamirs and their relation to Tibet, *Tectonics*, *23*, TC4002, doi:10.1029/2003TC001583.

Searle, M. P., and A. M. Khan (1996), *Geological Map of the North Pakistan and Adjacent Areas of Northern Ladakh and Western Tibet*, Scale 1:650,000, Oxford Univ. Press, Oxford.

Sippl, C., et al. (2013a), Geometry of the Pamir-Hindu Kush intermediate-depth earthquake zone from local seismic data, *J. Geophys. Res. Solid Earth*, *118*, 1438–1457, doi:10.1002/jgrb.50128.

Sippl, C., B. Schurr, J. Tympel, S. Angiboust, J. Mechie, X. Yuan, F. M. Schneider, S. V. Sobolev, L. Ratschbacher, and C. Haberland (2013b), Deep burial of Asian continental crust beneath the Pamir imaged with local earthquake tomography, *Earth Planet. Sci. Lett.*, *384*, 165–177, doi:10.1016/j.epsl.2013.10.013.

Sobel, E. R., L. M. Schoenbohm, J. Chen, R. C. Thiede, D. F. Stockli, M. Sudo, and M. R. Strecker (2011), Late Miocene-Pliocene deceleration of dextral slip between Pamir and Tarim: Implications for Pamir orogenesis, *Earth Planet. Sci. Lett.*, *304*(3–4), 369–378, doi:10.1016/j.epsl.2011.02.012.

Sobel, E. R., J. Chen, L. M. Schoenbohm, R. C. Thiede, D. F. Stockli, M. Sudo, and M. R. Strecker (2013), Oceanic-style subduction controls late Cenozoic deformation of the Northern Pamir orogen, *Earth Planet. Sci. Lett.*, *363*, 204–218, doi:10.1016/j.epsl.2012.12.009.

Stearns, M. A., B. R. Hacker, L. Ratschbacher, J. Lee, J. M. Cottle, and A. Kylander-Clark (2013), Synchronous Oligocene–Miocene metamorphism of the Pamir and the north Himalaya driven by plate-scale dynamics, *Geology*, *41*(10), 1071–1074, doi:10.1130/G34451.1.

Storchak, D. A., D. Di Giacomo, I. Bondár, E. R. Engdahl, J. Harris, W. H. K. Lee, A. Villaseñor, and P. Bormann (2013), Public release of the ISC-GEM global instrumental earthquake catalogue (1900–2009), *Seismol. Res. Lett.*, *84*, 810–815.

Strecker, M. R., W. Frisch, M. W. Hamburger, L. Ratschbacher, S. Semiletkin, A. Zamoruyev, and N. Sturchio (1995), Quaternary deformation in the Eastern Pamirs, Tadzhikistan and Kyrgyzstan, *Tectonics*, *14*(5), 1061–1079, doi:10.1029/95TC00927.

Stübner, K., L. Ratschbacher, D. Rutte, K. Stanek, V. Minaev, M. Wiesinger, and R. Gloaguen (2013a), The giant Shakhdara migmatitic gneiss dome, Pamir, India-Asia collision zone, I: Geometry and kinematics, *Tectonics*, *32*, 948–979, doi:10.1002/tect.20057.

Stübner, K., et al. (2013b), The giant Shakhdara migmatitic gneiss dome, Pamir, India-Asia collision zone, II: Timing of dome formation, *Tectonics*, *32*, 1404–1431, doi:10.1002/tect.20059.

Tapponnier, P., G. Peltzer, A. Le Dain, and P. Cobbold (1982), Propagating extrusion tectonics in Asia: New insights from simple experiments with plasticine, *Geology*, *10*, 611–616.

Thiede, R. C., E. R. Sobel, J. Chen, L. M. Schoenbohm, D. F. Stockli, M. Sudo, and M. R. Strecker (2013), Late Cenozoic extension and crustal doming in the India-Eurasia collision zone: New thermochronologic constraints from the NE Chinese Pamir, *Tectonics*, *32*, 763–779, doi:10.1002/tect.20050.

Trifonov, V. (1978), Late Quaternary tectonic movements of western and central Asia, *Geol. Soc. Am. Bull.*, *89*, 1059–1072.

Trifonov, V. G., V. I. Makarov, and S. F. Skobelev (1990), The Talas-Ferghana active right-lateral fault: Geotektonika [in Russian], no. 5, p. 18–92, *Geotectonics*, *24*(5), 435–442 (English).

van Hinsbergen, D. J. J., P. Kapp, G. Dupont-Nivet, P. C. Lippert, P. G. DeCelles, and T. H. Torsvik (2011), Restoration of Cenozoic deformation in Asia and the size of Greater India, *Tectonics*, *30*, TC5003, doi:10.1029/2011TC002908.

Vlasov, N. G., Y. A. Dyakov, and E. S. Cherev (Eds) (1991), *Geological Map of the Tajik SSR and Adjacent Territories, 1:500,000*, Vsesojuznoi Geol. Inst. Leningrad, Saint Petersburg.

Waldhauser, F., and W. L. Ellsworth (2000), A double-difference earthquake location algorithm: Method and application to the northern Hayward fault, California, *Bull. Seismol. Soc. Am.*, *90*(6), 1353–1368, doi:10.1785/0120000006.

Zanchi, A., M. Gaetani, S. Sironi, and S. Zanchetta (2011), Geological map of central-western Karakoram, Pakistan, 1:100,000, *It. J. Geosci.*, *130*(2), 161–162.

Zubovich, A. V., et al. (2010), GPS velocity field for the Tien Shan and surrounding regions, *Tectonics*, *29*, TC6014, doi:10.1029/2010TC002772.